

**Cell Chemical Biology, Volume 27**

**Supplemental Information**

**Site-Specific Photo-Crosslinking Proteomics**

**Reveal Regulation of IFITM3 Trafficking**

**and Turnover by VCP/p97 ATPase**

**Xiaojun Wu, Jennifer S. Spence, Tandriila Das, Xiaoqiu Yuan, Chengjie Chen, Yuqing Zhang, Yumeng Li, Yanan Sun, Kartik Chandran, Howard C. Hang, and Tao Peng**

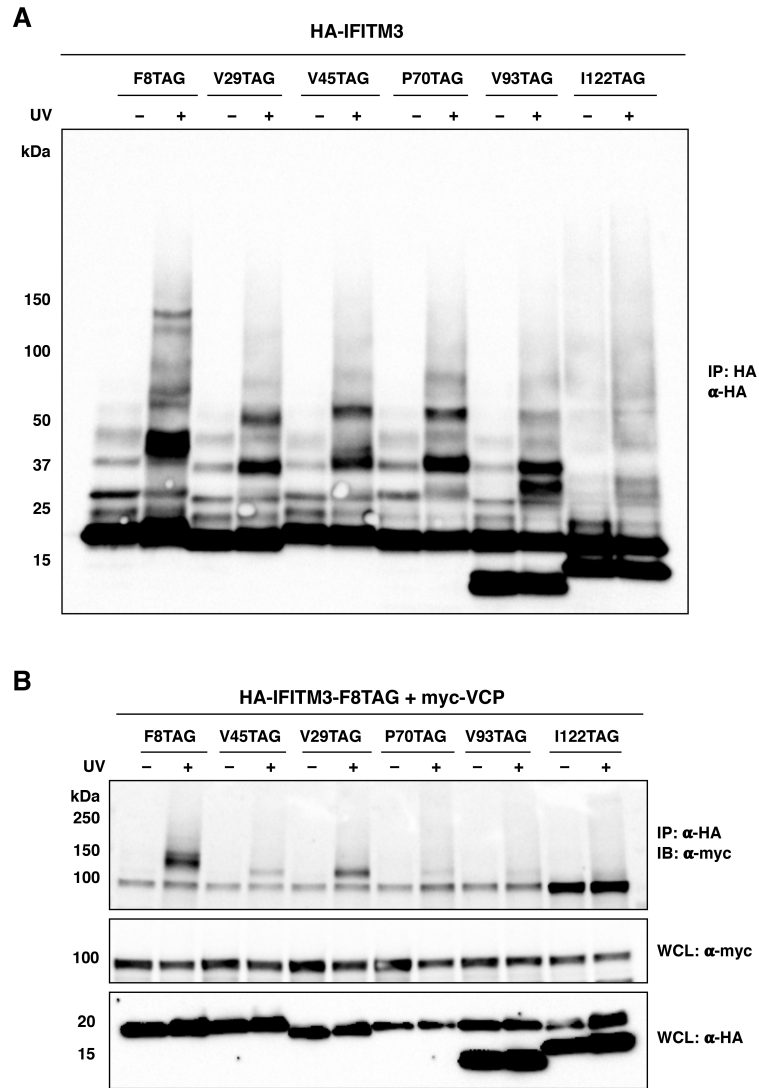


**Figure S1. Related to Figure 2 and Figure 3. Site-specific incorporation of DiZPK via amber suppression enables photo-crosslinking of IFITM3 with its interacting proteins.** (A) HEK293T cells transfected with HA-tagged IFITM3-TAG mutants of varying amber codon positions in the presence of DiZPK were irradiated with 365 nm light and subjected to anti-HA immunoprecipitation before Western blotting analysis. High molecular weight bands appeared in UV-irradiated samples indicate putative photo-crosslinked IFITM3 complexes. (B) HEK293T cells expressing HA-tagged DiZPK-modified IFITM3 of varying positions and myc-tagged VCP were UV irradiated and subjected to anti-HA immunoprecipitation for Western blotting analysis. The different intensities of photo-crosslinked bands suggest site-dependent photo-crosslinking efficiencies.

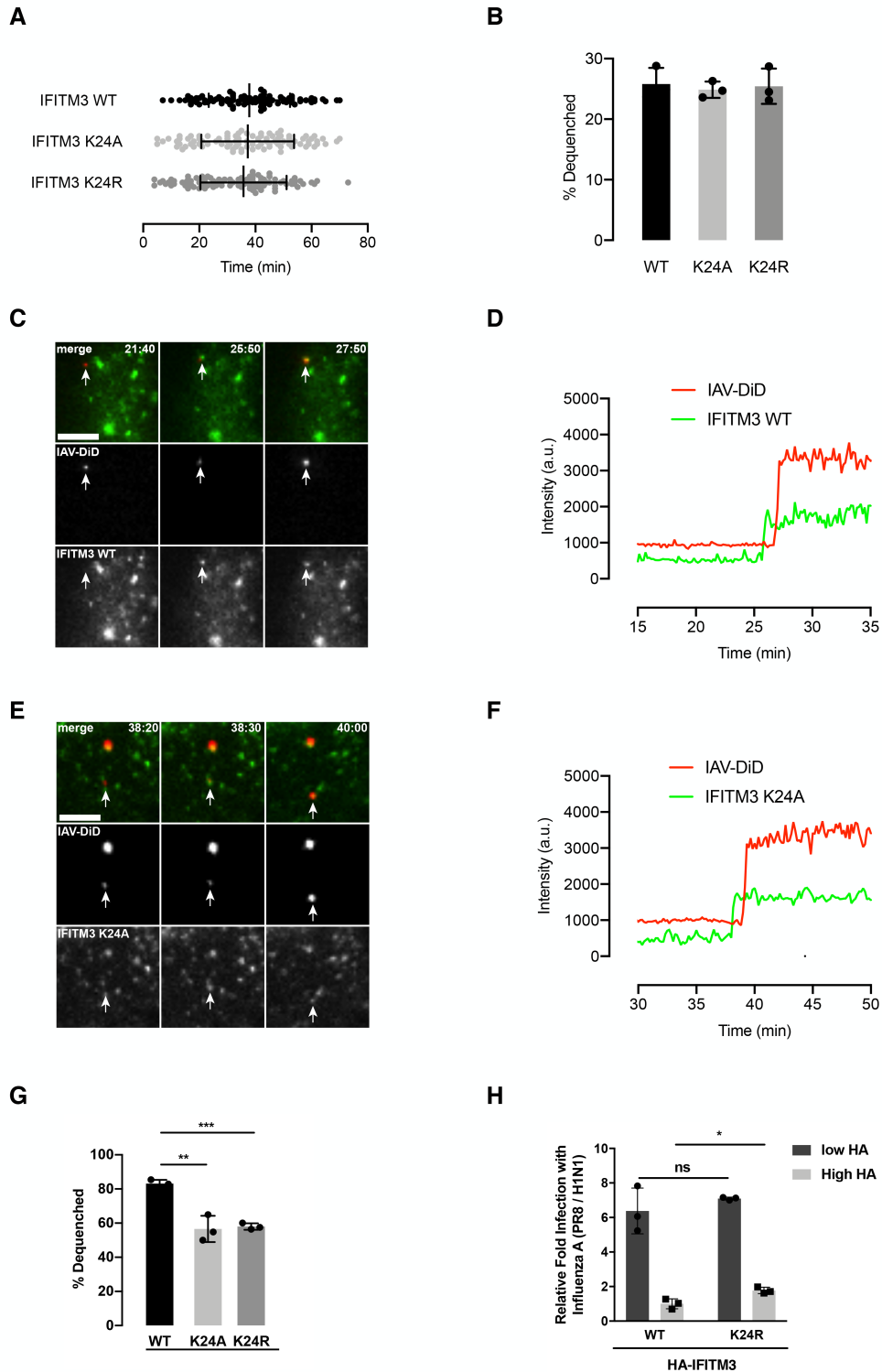


**Figure S2. Related to Figure 5. Live-cell imaging of IFITM3 co-trafficking with incoming DiD-labeled IAV particles and antiviral activity of IFITM3.** (A) Time of IAV fusion triggering events in HeLa cells expressing IFITM3 wild-type, K24A, or K24R. HeLa IFITM2/3 KO cells expressing BODIPY-labeled IFITM3 were infected with DiD-IAV particles and monitored for DiD-IAV dequenching and IFITM3 trafficking by time-lapse imaging as detailed in “Experimental Procedures”. Error bars represent mean and s.d.,  $n = 3$  independent experiments. (B) Total percentage of virus particles undergoing lipid mixing in cells expressing IFITM3 wild-type, K24A, or K24R. Error bars represent mean and s.d.,  $n = 3$ . (C) Example of lipid mixing in an IFITM3-positive compartment. (D) Fluorescence intensity

trace for the indicated particle shown in (C). (E) Example of lipid mixing in an IFITM3 K24A-positive compartment. (F) Fluorescence intensity trace for the indicated particle shown in (E). Scale bars = 5  $\mu\text{m}$ . (G) Relative percentage of DiD-IAV particles colocalized with IFITM3, K24A, or K24R mutant at the time of dequenching. Related to Figure 5E. Data represent the mean and s.d. of three independent experiments. \*\* and \*\*\* indicate p-values  $<0.01$  and  $<0.001$ , respectively, calculated by Student's t-test. (H) Antiviral activity of IFITM3 wild-type, K24A, and K24R mutants assayed by flow cytometry. Related to Figure 5F. "Low HA" and "High HA" indicate cell populations expressing low and high levels of HA-IFITM3, respectively. Data represent the mean and s.d. of three independent experiments. \* indicates a p-value  $<0.1$  and ns indicates a p-value  $>0.05$  calculated by Student's t-test.



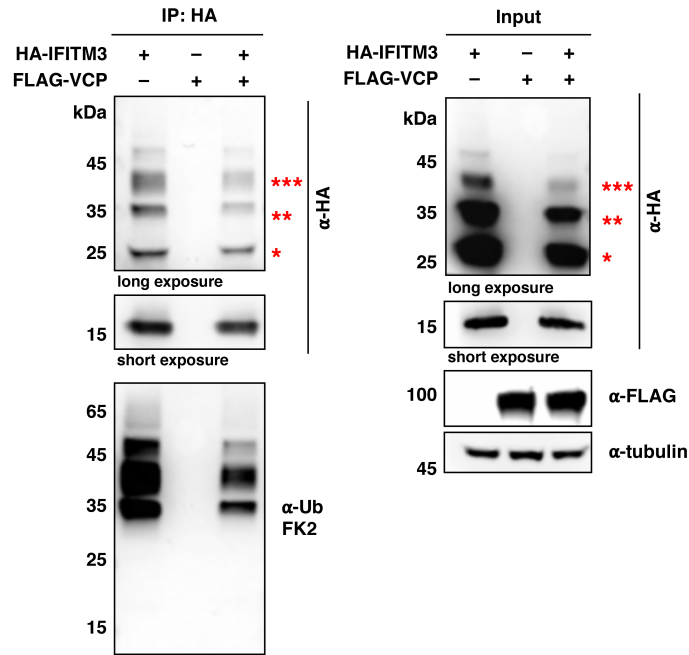


**Figure S3. Related to Figure 6. Overexpression of VCP results in decreased levels of both non-ubiquitinated and ubiquitinated IFITM3.** HEK293T cells were transfected with HA-tagged IFITM3 and/or FLAG-tagged VCP, and cell lysates were immunoprecipitated with anti-HA resin for Western blotting analysis with an anti-HA or anti-ubiquitin antibody. The red asterisks indicate the IFITM3 ubiquitination bands with high molecular weights. Western blots of cell lysates with anti-HA and anti-FLAG antibodies were performed to confirm protein expression, and anti-tubulin Western blotting was performed to confirm comparable protein loading.

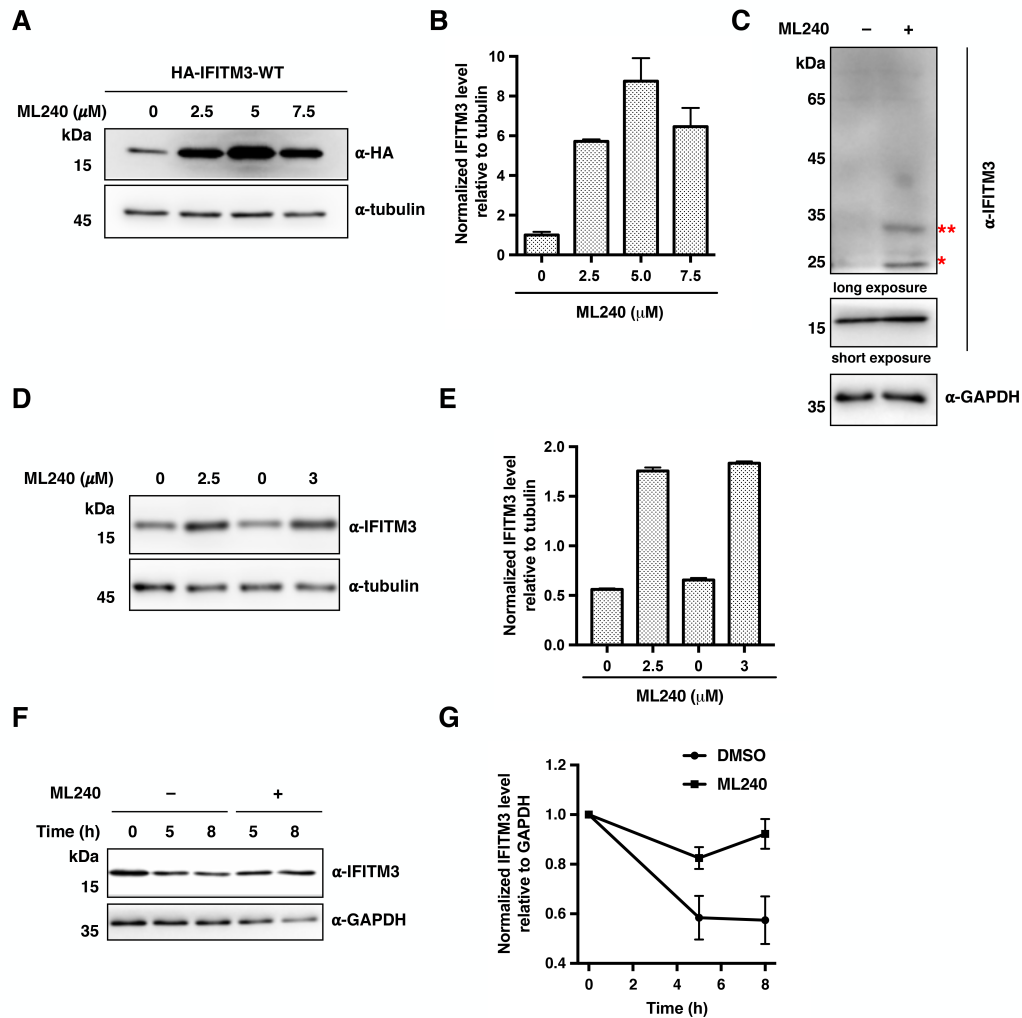


**Figure S4. Related to Figure 7. Chemical inhibition of VCP with ML240 leads to accumulation and delayed degradation of IFITM3.** (A) Western blotting analysis of IFITM3 levels upon treatment with ML240. HeLa cells were transfected with wild-type IFITM3 for 25 h, treated with ML240 at indicated concentration for another 9 h, and then lysed for anti-HA Western blotting analysis. Anti-tubulin blots served as loading controls. (B) Quantification of IFITM3 levels normalized to tubulin levels shown in (A). Data are represented as mean  $\pm$  s.d.,  $n = 3$ . (C) Ubiquitination level of endogenous IFITM3 increases upon ML240 treatment. HeLa cells were treated with ML240 (5  $\mu$ M) for 12 h and lysed for anti-IFITM3 Western blotting analysis. The red asterisks indicate the IFITM3 ubiquitination bands with high molecular weights. (D) Western blotting analysis of endogenous IFITM3 upon treatment with ML240. HeLa cells were treated with ML240 at indicated concentration for 24 h and lysed for anti-IFITM3 Western blotting analysis. The anti-tubulin blot served as loading controls. (E) Quantification of IFITM3 levels normalized to tubulin levels shown in (D). Data are represented as mean  $\pm$  s.d.,  $n = 3$ . (F) Western blotting analysis of endogenous IFITM3 turnover in the presence of ML240. HeLa cells were treated with CHX (25  $\mu$ g/ml) for indicated time in the presence of DMSO or ML240 (2.5  $\mu$ M) and lysed for anti-IFITM3 Western blotting analysis. The anti-GAPDH blot served as loading controls. (G) Quantification of IFITM3 levels normalized to GAPDH levels shown in (F). Data are represented as mean  $\pm$  s.d.,  $n = 3$ .

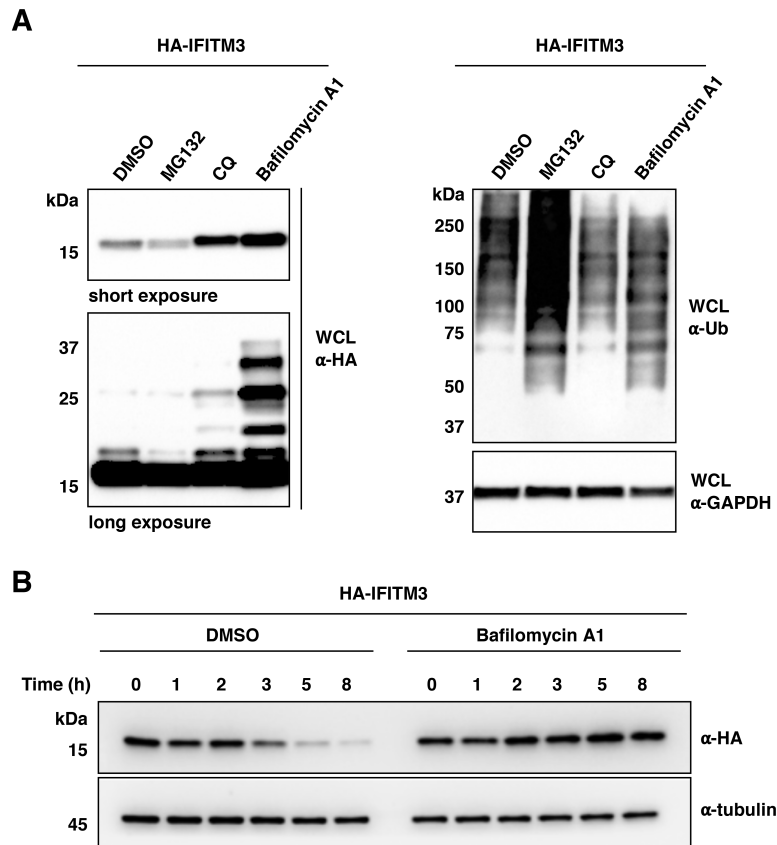


**Figure S5. Related to Figure 7. Western blotting analysis of IFITM3 level and turnover upon pharmacological treatments.** (A) Western blotting analysis of IFITM3 and ubiquitination levels upon treatment with proteasome or lysosome inhibitors. HEK293T cells were transfected with wild-type HA-IFITM3 for 16 h and treated with DMSO, MG132 (50  $\mu$ M), CQ (100  $\mu$ M), or Bafilomycin A1 (100 ng/mL) for another 12 h. Cells were then lysed for anti-HA Western blotting analysis. Western blots of cell lysates with anti-ubiquitin and anti-tubulin antibodies were performed to confirm protein ubiquitination levels and comparable sample loading, respectively. (B) Turnover of IFITM3 in the presence of Bafilomycin A1. HeLa cells expressing wild-type IFITM3 were treated with CHX (25  $\mu$ g/ml) for indicated time in the presence of DMSO or Bafilomycin A1 (100 ng/mL) and lysed for anti-HA Western blotting analysis. Anti-tubulin blots served as loading controls.

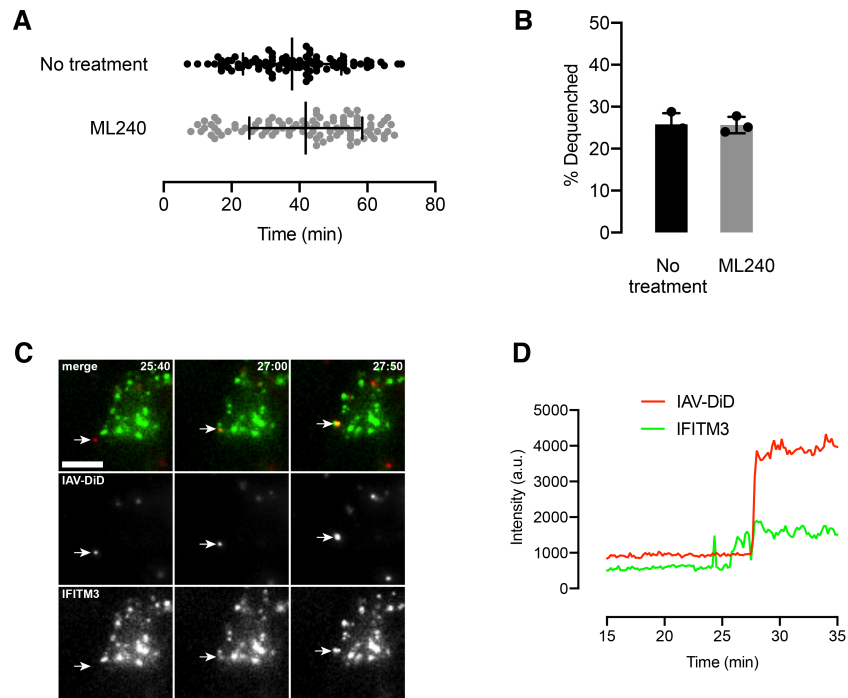


**Figure S6. Related to Figure 7. Live-cell imaging of IFITM3 co-trafficking with incoming DiD-labeled IAV particles in the presence of ML240.** (A) Time of IAV fusion triggering events in HeLa cells expressing wild-type IFITM3 in the presence of ML240. HeLa IFITM2/3 KO cells expressing BODIPY-labeled IFITM3 were infected with DiD-IAV particles, treated with ML240, and monitored for DiD-IAV dequenched and IFITM3 trafficking by time-lapse imaging as detailed in “Experimental Procedures”. Error bars represent mean and s.d.,  $n = 3$  independent experiments. (B) Total percentage of virus particles undergoing lipid mixing in cells expressing wild-type IFITM3 in the presence of ML240. Error bars represent mean and s.d.,  $n = 3$ . (C) Example of lipid mixing in an IFITM3-positive compartment upon ML240 treatment. (D) Fluorescence intensity trace for the indicated particle shown in (C). Scale bars = 5  $\mu\text{m}$ .

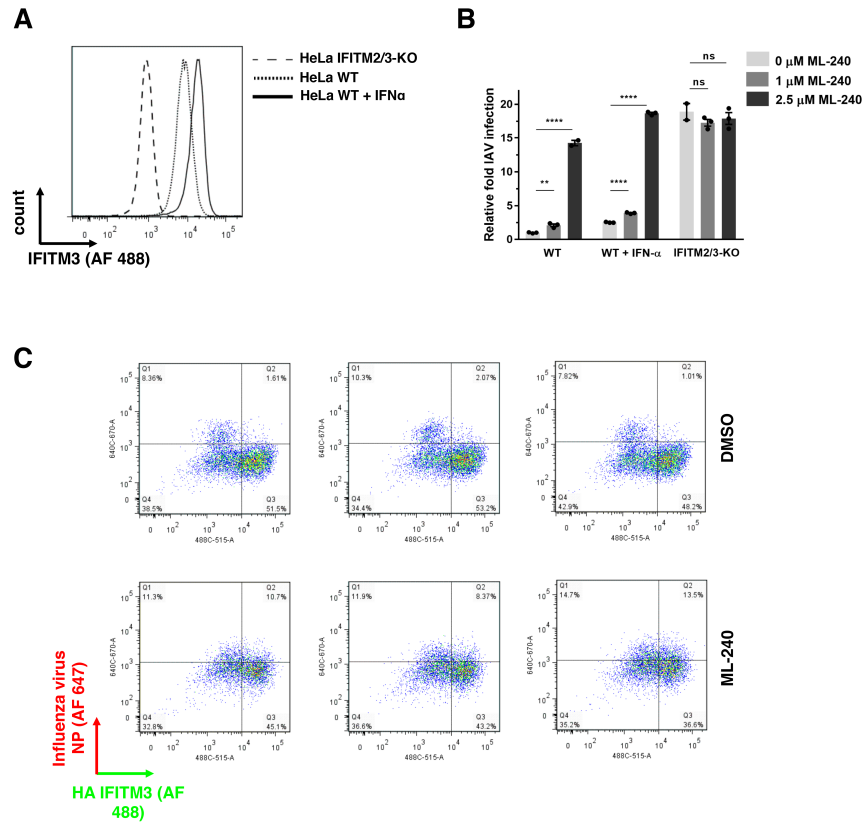


**Figure S7. Related to Figure 7. IFITM3 expression and virus infection in naïve, IFN $\alpha$  stimulated HeLa WT and IFITM2/3-KO cell lines upon ML240 treatment. (A)** Expression level of IFITM3 in naïve, IFN $\alpha$  stimulated HeLa WT and IFITM2/3-KO cell lines assayed with flow cytometry. **(B)** IAV infection of naïve, IFN- $\alpha$  stimulated HeLa WT and IFITM2/3-KO cell lines upon acute treatment with ML240. Cells were stimulated with 1:1000 of IFN- $\alpha$  (100  $\mu$ g/mL) for 16 h, followed by infection with IAV (MOI = 2.5). At 2 h post-infection, cells were treated with ML240. After 4 h, cells were harvested, stained for IAV nucleoprotein (NP), and analyzed by flow cytometry. The percentage of NP-positive cells was normalized to untreated WT cells and plotted as relative infection fold. Data represent the mean and standard error of mean from three independent experiments (\*\* p < 0.01, \*\*\*\* p < 0.0001. p-values were calculated by Student's t-test). **(C)** Scatter plots of antiviral activity assay shown in Figure 7F. HeLa IFITM2/3 KO cells transfected with HA-IFITM3 were infected with IAV (PR8/H1N1) at an MOI of 2.5 for 2 h. Cells were then treated with ML240 (2.5  $\mu$ M) for 4 h and fixed for staining with anti-influenza virus NP and anti-HA antibodies to measure the percentage of cells expressing IFITM3 and/or infected using flow cytometry. Identical gating for anti-HA and anti-NP signals was used.